Chapter 5

Functionalized novolac-based polymer- silver nanoparticles hybrid:

An effective antibacterial material

5.1 Introduction

Enriched with outstanding properties, hybrid materials of polymers with silver nanoparticles (AgNPs) emerged interesting and promising systems for a wide range of biocidal applications. Highlights of AgNPs and their antimicrobial efficacy are presented in *Chapter-1*, with attention on their incorporation in polymer support matrix developing antimicrobial hybrid materials. Phenolic resins are relatively inexpensive and three-dimensional synthetic polymers that have attracted scientific and industrial interests for broad array of applications as illustrated in *Chapter-1*. Quite surprisingly, to the best of our knowledge, the use of phenolic resin-based materials for antibacterial applications remains almost untouched. Thus, achieving an antibacterial property for AgNPs when embedded in phenolic resin is an attractive challenge. In this context, novolac type phenolic epoxy resin, which contributed to the inventory of azo dye adsorbing materials as described in Chapters 2 – 4, offers new avenues to design support materials for AgNPs in the development of bactericides for healthcare applications. This chapter is based upon our publication[5.1] focusing on novolac type phenolic resin support for AgNPs to exhibit antibacterial activity.

5.2 Objective

The attention of this chapter is drawn to the simple preparation of hybrid **5.3** derived from functionalized novolac resin **5.1** and AgNPs as illustrated in Figure 5.1. The prepared hybrid held the antibacterial activity against Gram-positive bacteria and Gram-negative bacteria. According to our best knowledge, this is the first report describing functional novolac-AgNPs hybrid being exploited in the context of combating bacteria.

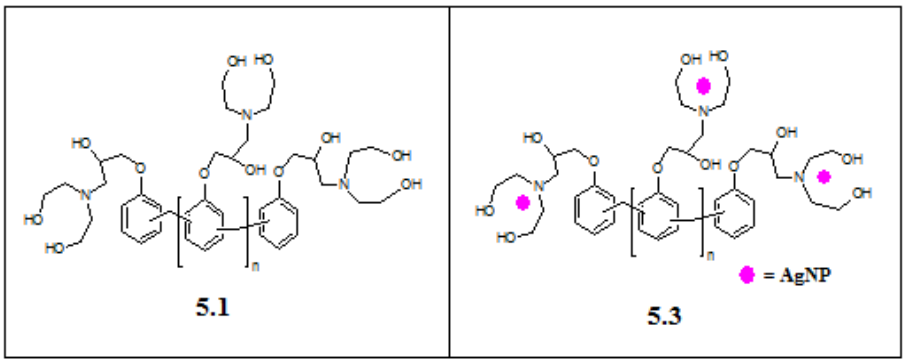

Figure 5.1 The structures of fuctionalized novolac resin **5.1** and its hybrid with AgNPs **5.3**

5.3 Experimental Section

5.3.1 Materials and Measurements

Novolac-based epoxy resin precursor **2.2** was prepared according to the procedure reported in Chapter 2. NMR spectra were recorded on a Brucker NMR spectrometer. FTIR spectrum was recorded on Perkin Elmer spectrophotometer using KBr pallet. Thermal (TGA) analysis was conducted with Perkin Elmer STA 6000 instrument under nitrogen atmosphere. UV-vis

spectra were recorded on Shimadzu UV-1800 spectrophotometer. Transmission Electron Microscopy (TEM) was used to determine the particles size. High resolution JEOL JEM1400 plus, 120KeV instrument was used for TEM analysis. Small amount of DMSO-water solution of **5.3** was dispersed in acetone. A drop of thin dispersion was placed on carbon coated copper grid, dried and examined in the transmission electron microscope.

5.3.2 Synthesis of functionalized novolac resin 5.1

To the epoxy resin **2.2** (M_w = 3300, MWD 1.10) (0.45g) diethanolamine (2.1g, 20.0 mmol) was added. The reaction mixture was heated with stirring at 95-100^{o}C for 4h. The product was precipitated as gummy solid with plenty of water. Precipitate was collected and vacuum dried at 60 ^{0}C for 24h. FTIR (KBr): ν_{max} = 3433, 2905, 1610, 1509, 1453, 1334, 1243, 1174, 1113, 1036, 880, 811, 754 cm^{-1}; ^{1}H NMR (DMSO-d_6, 300MHz) δ: 7.29 (bm, ArH), 7.08 (bm, ArH), 6.91 (bm, ArH), 6.82 (bm, ArH), 5.39 (bs, -OH), 4.78 (bs, -OH), 4.38 (bs, -OH), 3.98-3.70 (bm, $ArOCH_2$-, $Ar\text{-}CH_2$-), 3.56-3.35 (bm, $Ar\text{-}CH_2$-, $-NCH_2CH_2OH$), 2.58 (m, $-NCH_2CH_2OH$).

5.3.3 Preparation of functionalized novolac resin-silver nanoparticles hybrid

Solution of **5.1** (3.58 mg / ml) in DMSO was mixed with aqueous solution of $AgNO_3$ (6.38 mM) in the ratio of 20:1 (v/v). The mixture was stirred for 30 min at ambient temperature followed by the gradual addition of freshly

prepared aqueous solution of $NaBH_4$ (1.2 g/L) (1:5, v/v with respect to $AgNO_3$ solution) under vigorous stirring. The color of the mixture turns from light yellow into reddish violet to yield the composite **5.3** and the resultant mixture was maintained stirring for 1 h.

5.3.4 Antimicrobial assay

The antibacterial screening of **5.3** was carried out against Gram-positive bacteria, *Staphylococcus aureus* MTCC 3160, *Staphylococcus epidermidis* NCIM2493, *Bacillus subtilis* and Gram-negative bacteria, *Pseudomonas aeruginosa* ATCC27853, *Escherichia coli* using agar well diffusion assay according to reported procedures[5.2-5.4]. Briefly, the test pathogen was spread on agar test plate with the help of a spreader. Then circular wells were made with a sterilized steel borer in each plate. 30 µl of the prepared solution of **5.3** as mentioned was placed on wells of agar plates seeded with bacterial strains. Similar experiment was also carried out with the solution of **5.1** alone and was used as a control. After 24 h incubation at 37°C, the zones of inhibitions were noted. Minimum inhibitory concentration (MIC) values of **5.3** against the pathogens were determined by broth micro-dilution method following Clinical and Laboratory Standards Institute (CLSI) guidelines[5.5,5.6]. MIC values were determined where no visible growth was observed. Different concentrations of **5.3** ranging from 0.48 µL to 1 mL were added to sterile 96-well microtitre plates in a serial dilution manner and the volume was made up to 200 µL/ well with respective medium containing a total inoculums load of ca. 10^5 cells/well.

Finally, microtitre plates were incubated at 37°C. DMSO-water (20:1, v/v) solution of **5.1** was used and cultured under the same condition as the control test. Bacterial growth curve study was considered to determine the killing kinetics in which two experimental set ups were designed. In the first experimental set up, *S. aureus* and *P. aeruginosa* were grown in Muller Hinton Broth (MHB). The absorbance of bacterial suspension was measured for 600 hours at 600 nm. All experiments were repeated thrice.

5.3.5 Cytoplasmic material release assay

Cytoplasmic material release study was performed following the reported procedure[5,7]. Briefly, 1 mL of bacterial (*P. aeruginosa* and *S. epidermidis*) culture (0.5×10^7 CFU/ mL) were centrifuged, pellet was washed with PBS (1X) buffer and suspended in same buffer. Aliquots of 200 μL of suspended solution were used for further analysis. Different aliquots of cell suspensions were treated with fixed concentration at 4.0 μL of both **5.1** and **5.3**, separately at 30°C for 12 h. The samples were filtered to remove bacteria cells, and optical density (OD) of supernatants was recorded at 260 nm. The percentage of cytoplasmic material release was quantified considering the OD values obtained with Triton X-100 (0.1%) treatment with 100% release. All the experiments were repeated three times.

5.4 Results and discussion

5.4.1 Synthesis and characterization of functionalized novolac resin

Because of the ligation chemistry, diethanolamine was chosen as anchoring motif in modifying novolac epoxy resin **2.2**. In view of this, epoxy resin **2.2** was covalently functionalized with diethanolamine by ring opening reaction to reach functionalized novolac polymer **5.1** as outlined in Scheme 5.1.

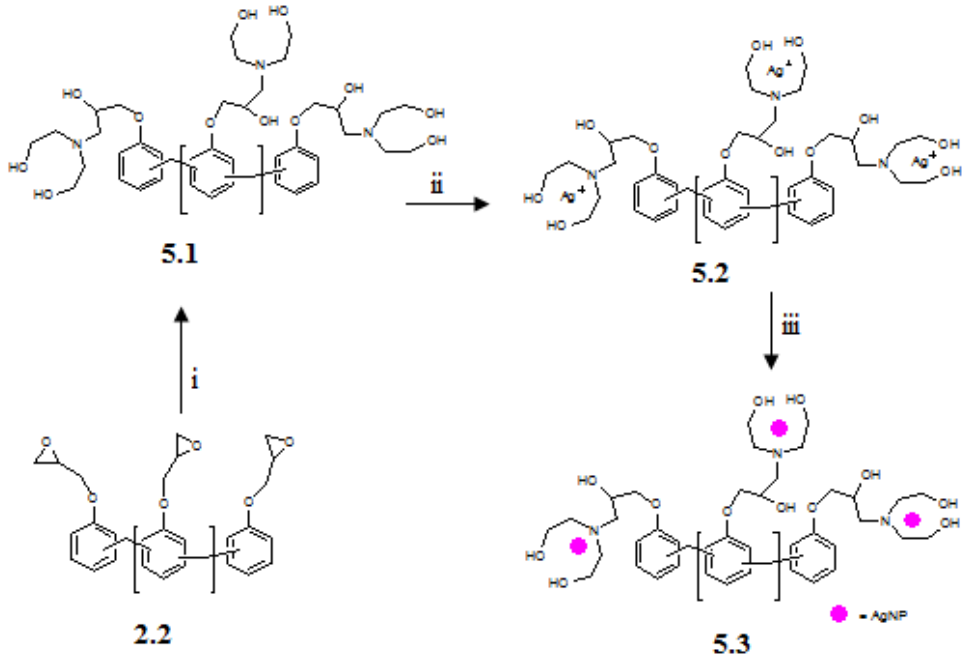

Scheme 5.1 Synthesis of hybrid **5.3**: (i) Diethanolamine, 110^{o}C, 4h (ii) $AgNO_3$ (iii) $NaBH_4$

Chapter 2 described the preparation and characterization of epoxy resin precursor **2.2**. Prepared polymer **5.1** was characterized by FTIR, ^{1}H NMR spectroscopy and thermal (TGA) analysis. In the FTIR spectrum of **5.1** (Figure 5.2) the broad absorption band that appears at 3433 cm^{-1} was assigned

to O-H stretching frequency. The less intense absorption band at 2905 cm^{-1} could be assigned to the aliphatic C–H stretching vibration. The absence of epoxy-associated peak at 904 cm^{-1} indicates the extent of reaction. Further, peaks assigned at 1235 and 1069 cm^{-1} were attributed to C–N stretching possibly due to the presence of amino groups.

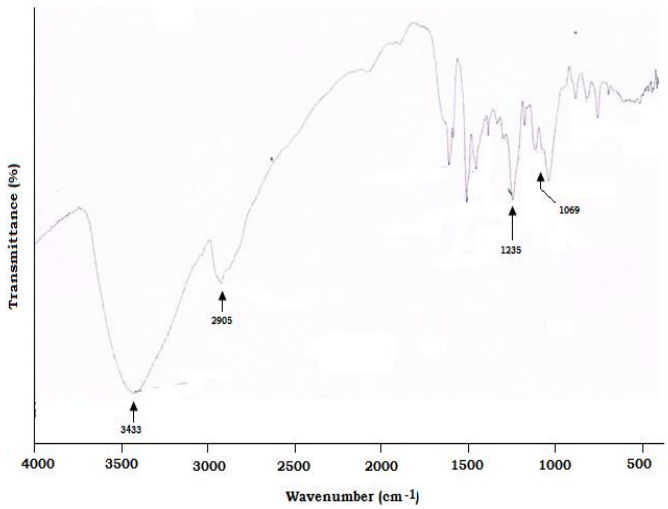

Figure 5.2. FTIR spectrum of **5.1**

The completion of reaction could be indicated by the disappearance of epoxy protons signals in the region 2.86 - 2.70 ppm. The broad resonance signals in the region 7.30 – 6.82 ppm due to the aromatic protons confirms the existence of novolac skeleton (Figure 5.3).

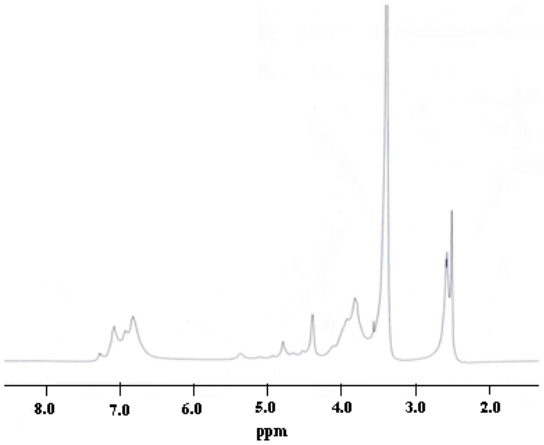

Figure 5.3. ^{1}H NMR spectrum of **5.1**

Thermal stability of **5.1** was estimated using TGA analysis. The results are summarized in Table 5.1. Polymer **5.1** showed thermal stability of up to 175 ^{o}C with ~10% weight loss in nitrogen due to the presence of moisture. While it experienced two stages weight loss events from 175 to 500 ^{o}C. This may be ascribed to the degradation of polymer skeleton.

Table 5.1. Thermal (TGA) properties of **5.1**

Polymer	T_d^{10}(^{o}C)	Stage	Temp range (^{o}C)	Weight loss %	Y_c at 500 ^{o}C (wt%)
5.1	175	1 2	175-345 345-500	37.0 29.75	26.8

TGA was performed at a heating rate of 5^{0}C / min under nitrogen flow; T_d^{10} = Temperature at which 10% weight loss occurred; Y_c = char yield.

This thermal stability will surely be an added advantage of combining **5.1** with other matrices by standard processing condition, which would have potential value in the production of new antibacterial materials**.**

5.4.2 Characterization of functionalized novolac resin-AgNPs hybrid

It is expected that the macromolecular framework **5.1** with a number of easily accessible functional groups can provide a particular benefit through chelation of Ag^+ ion with subsequent nucleation site for AgNPs. To this end an aqueous solution of $AgNO_3$ was added to the DMSO solution of **5.1** following reduction with very dilute aqueous solution of $NaBH_4$ at room temperature to produce **5.3**. The immediate color change from faint yellow to reddish-brown as shown in Figure 5.4 suggested the successful formation of AgNPs. The solution was stable for several weeks at room temperature without any special attention. Hybrid **5.3** was characterized by UV-vis and TEM analyses. Reduction resulted in the appearance of a high intensity surface plasmon resonance (SPR) band[5.8-5.10] centered at 440 nm indicating the formation of AgNPs (Figure 5.5). In addition, no signature peak at a higher wavelength points toward the absence of the large aggregation of Ag NPs[5.11,5.12]. No noticeable precipitate was observed upon addition of aqueous solution of Na_2S evidencing complete conversion of Ag^+ to Ag NPs.

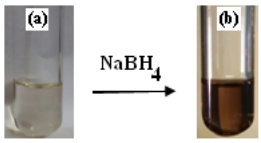

Figure 5.4. Digital optical images showing color of the solutions of (a) **5.2** and (b) **5.3** in DMSO-water (20:1, v/v) ([$AgNO_3$] = 6.38 mM).

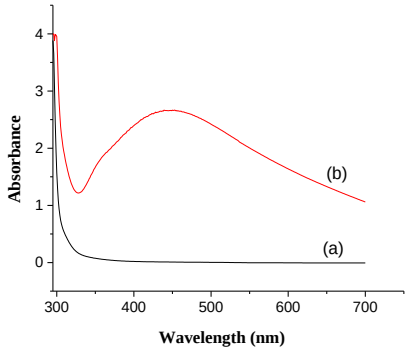

Figure 5.5. UV-vis spectra of (a) **5.2** and (b) **5.3** in DMSO-water (20:1, v/v) ([$AgNO_3$] = 6.38 mM).

It is worth mentioning that the particle size is an important parameter which determines the antimicrobial effectiveness of the resultant nanoparticles[5.13-5.16]. Thus, prior to the antibacterial studies, we examined the particle sizes of the formed AgNPs. Figure 5.6 shows TEM micrograph and the particle size distribution histogram of AgNPs formed. The image shows roughly spherical-like shape of AgNPs dispersed in the polymer matrix. The histogram illustrates the somewhat wide size distribution ranging from 3 nm to 22 nm in diameter. It is also noted that the majority of particles were in the range of 7 nm to 12 nm in diameter which supports to the symmetric shape of SPR band

in the UV-visible spectrum. Besides, the appearance of very few elongated irregular shaped nanoparticles was noted. Taken together, UV-vis and TEM observations are in close agreement with the earlier reported study on AgNPs embedded into poly(vinyl alcohol) film[5.17].

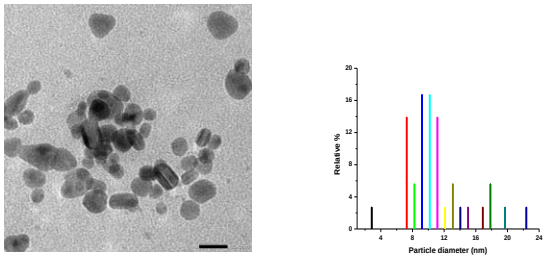

Figure 5.6. TEM image and corresponding histogram of **5.3**

5.4.3 Antibacterial Assay

Hybrid **5.3** showed remarkable activity against both Gram-positive and Gram-negative bacteria as evaluated using both disc diffusion and MIC methods. **5.3** displayed distinct inhibition zones against both gram-positive and gram-negative bacterial strains. As a representative example, the agar diffusion assay plates against different bacterial strains like *Staphylococcus aureus*, *Bacillus subtilis* and *Escherichia coli* toward **5.3** is presented in Figure 5.7. As a control, solution of **5.1** in DMSO-water (20:1, v/v) showed no inhibitory effect.

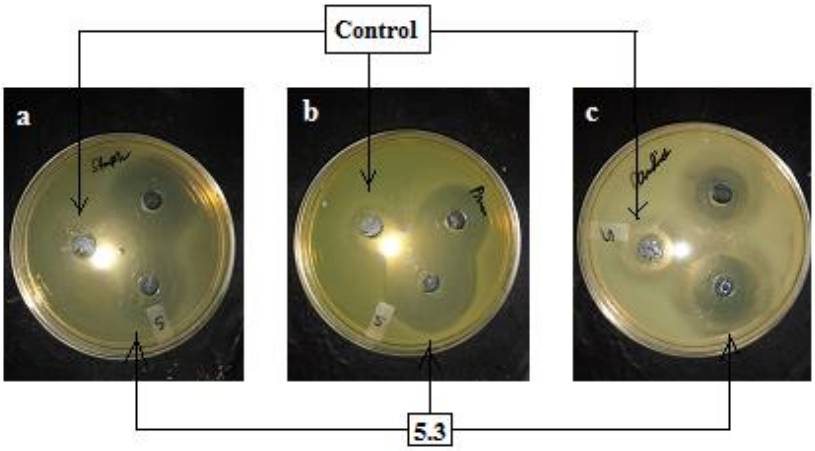

Figure 5.7. Images showing inhibitory zones of **5.3** hybrid against (a) *Staphylococcus aureus* (b) *Bacillus subtilis* and (c) *Escherichia coli* on agar plates.

The observed MIC values are listed in Table 5.2. Among the tested bacteria, the lowest inhibitory effect was noted for P. aeruginosa with the maximum MIC of 7.81 µL. From the results it is evident that the selected pathogens were susceptible to **5.3**.

Table 5.2. MIC values (µL) of **5.1** and **5.3** with AgNPs loading amount (µg)

Bacteria	Functionalized novolac resin **5.1**	Hybrid **5.3** (µL) (AgNPs loading (µg))
P. aeruginosa	nd	7.81 µL (5.32 µg)
E. Coli	nd	3.90 µL (2.65 µg)
S. aureus	nd	3.90 µL (2.65 µg)
S. epidermides	nd	3.90 µL (2.65 µg)
B. subtilis	nd	1.95 µL (1.33 µg)

nd = no detectable MIC

Not only inhibition, the bacterial killing activity of **5.3** was also noticed. Killing-curve assay revealed its strong bactericidal activity (Figure 5.8) and no cells become started to grow within 600 h. Moreover, the killing activity of **5.3** against S. aureus and P. Aeruginosa was almost identical. The results thus accounted for the prolonged inhibitory effect of **5.3** on the bacterial growth. As reported in literature[5.7], the release of cytoplasmic materials is a marker of the damage in the bacterial cytoplasmic membrane. Remarkable leakage of cytoplasmic materials was observed upon exposure of selected strains to **5.3** (Figure 5.9) evidencing nanoparticle mediated membrane damage. The results further demonstrated that the release of cytoplasmic material was more for *S. aureus* strain in comparison to *P. aeruginosa* strain implying greater membrane damage. This could be due to the difference in cell wall composition between Gram-positive and Gram-negative bacteria protecting against antibacterial material[5.18]. It is worth noting that the extent of membrane damage and cytoplasmic contents leakage correlates with the observed difference in MIC values of bacterial strains.

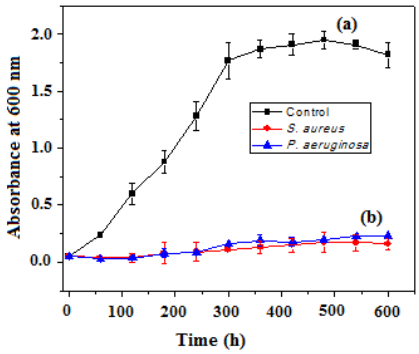

Figure 5.8. Growth curves of representative pathogenic microorganisms exposed to (a) **5.1** and (b) **5.3**. Amount of hybrid **5.3** used in this assay as the obtained MIC values.

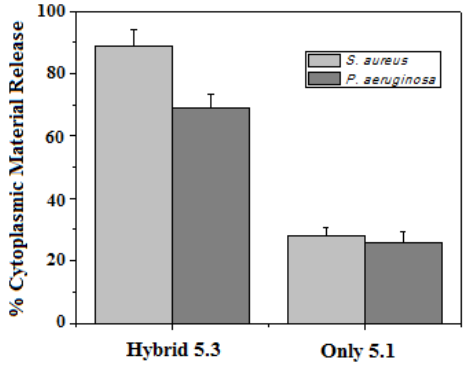

Figure 5.9. Bar graph showing the effect of **5.3** and **5.1** on the release of cytoplasmic material. The bacteria were incubated with a fixed concentration (4.0 µL) at 30°C for 12 h. The change in the absorbance at 260 nm was monitored. Data are the mean of triplicates ± S.E.

Although the exact mechanism is not entirely understood, available reports in the literature[5.19] described the possible mechanisms of bactericidal effect of AgNPs. The interaction of AgNPs with the building elements of the bacterial membrane eventually leads to increased membrane permeability and resulting in death of cell. Other studies suggested that AgNPs appear to penetrate inside the cell, where they further interact with phosphorus moieties in DNA and

react with sulfur-containing proteins. This could lead to inhibition of enzyme functions and interruption of DNA replication resulting in cell death[5.20-5.23] . Other mechanism involving the release of silver ions by AgNPs is also believed for bactericidal effect[5.20]. Meanwhile, the size and shape of AgNPs are reported to have influences on antibacterial efficacy[5.13-5.16]. The spherical and smaller sized AgNPs have larger specific surface area for interaction with the cell surface improving antibacterial effectiveness. The observations noted in our study suggest that hybrid **5.3** could induce the release of cytoplasmic materials by increasing the membrane permeability leading to disruption of cellular processes. This membrane damaging mechanism is similar to reported literature[5.7]. Macromolecular framework bearing abundant hydroxyl and amino groups further ensures complete protection and prevents aggregation of spherical-like nanoparticles providing efficient antimicrobial activity. Thus the **5.3** appears to have potential for use as a long-term antibacterial agent.

5.5 Conclusion

This chapter gives an account for the facile preparation of hybrid **5.3** of functionalized novolac resin with AgNPs. The antibacterial experiment demonstrated good activity of **5.3** against Gram-positive bacteria, Staphylococcus aureus MTCC 3160, Staphylococcus epidermidis NCIM2493, Bacillus subtilis and Gram-negative bacteria, Pseudomonas aeruginosa ATCC27853, Escherichia coli. The minimum inhibitory concentration (MIC)

was determined. Hybrid showed excellent antibacterial activity against both Gram-positive and Gram-negative bacteria. The antibacterial mechanism investigation indicated the membrane damaging action leading to the release of cytoplasmic materials and the death of the pathogen.

5.6 Further scope of work

The author recommends further research:

i) Adequate functionality in processable **5.3** can be a source of hydrogen bonding additive in polymer blending. This might provide durable antibacterial functionalization of novolac-based new easy-to-handle blend materials which may offer possibility for practical applications in human health associated sectors including antimicrobial surface coating and packaging.

ii) Functional groups in **5.1** explain its ability to complex with silver salts. Further chemical modification like crosslinking of **5.1** is expected to open new avenues in developing AgNPs loaded antibacterial network materials, which enables one to introduce special properties and direct them for healthcare applications including microbial decontamination of water.